

# A STUDY ON THERMAL DIFFUSION AND CHEMICAL REACTION ON PULSATILE FLOW OF A DUSTY FLUID THROUGH AN IRREGULAR CHANNEL IN THE PRESENCE OF POROUS MEDIUM

## K. R. Madhura\* & G. Kalpana\*\*

\* Post Graduate Department of Mathematics, The National College, Bangalore, Karnataka & Trans - Disciplinary Research Centre, National Degree College, Basavanagudi and The Florida International University, United States of America

\*\* Department of Mathematics, Sri Krishna Institute of Technology, Bangalore, Karnataka & Research Scholar, East West Institute of Technology, VTU, Karnataka

**Cite This Article:** K. R. Madhura & G. Kalpana, "A Study on Thermal Diffusion and Chemical Reaction on Pulsatile Flow of a Dusty Fluid through an Irregular Channel in the Presence of Porous Medium", International Journal of Advanced Trends in Engineering and Technology, Volume 2, Issue 2, Page Number 204-214, 2017.

#### **Abstract:**

This article presents the consequences of flow of a dusty fluid between two vertically heated, porous, irregular channel. The governing equations of the above problem are set up and non dimensionalised. The non dimensional governing equations are solved analytically by variable separable method and Laplace transform method and numerically by Crank Nicolson and finite difference methods. The velocity, temperature and concentration fields have been studied and graphical results are presented and physical aspects are discussed in detail to interpret the effect of various physical parameters of the problem.

**Key Words:** Dusty Fluid, Heat Transfer, Chemical Reaction, Irregular Channel & Pulsatile Flow **1. Introduction** 

Heat transfer effects on dusty fluid flow takes an significant role in fluid mechanics due to its vast applications in many fields like polymer technology such as glass fiber production, extrusion of polymer in melt-spinning process and many others. Sustain plasma confinement for controlled thermo nuclear fusion, electromagnetic casting of metals, liquid metal cooling of nuclear reactions, etc. are the few areas which requires to analyze the effect of thermal diffusion and chemical reaction. Om prakash, et al. [1] have considered Walter's liquid model-B to investigate the effect of chemical reaction and thermal diffusion on the unsteady dusty flow of an incompressible, visco-elastic fluid between two heated porous infinite parallel plates. Effects of thermal diffusion and diffusion thermo on heat and mass transfer of steady, incompressible, electrically conducting fluid was discussed in [2] and [3]. G. Palani and P. Ganesan [4] have numerically studied the effects of heat transfer on the flow of dusty gas past a semi-infinite isothermal inclined plate. The two dimensional, MHD flow, heat and mass transfer of a viscous fluid over a incessantly moving porous surface inserted in a Darcian porous medium under soret and dufour effect was examined in [5] and [6]. Two dimensional laminar boundary layer flow and heat transfer of a steady/unsteady, incompressible, viscous dusty fluid over a stretching sheet was explained in [7] and [8]. The effects of heat source or sink on the MHD boundary layer flow and heat transfer over a porous shrinking sheet with mass suction are investigated by K.Bhattacharya [9]. P.V.S. Kamalakar et al. [10] have studied thermo diffusion effect through a porous medium on non-Darcy convective heat and mass transfer flow of a viscous fluid in a vertical channel with heat generating sources using finite element analysis.

G.K. Ramesh and B.J. Gireesha [11] have got the numerical solution for the heat transfer of dust fluid and radiation effect of boundary layer flow over a stretching sheet taking into an account of non-uniform heat source/sink. P. Mohan krishna et al. [12] have found the analytical solution of a dusty viscous fluid of the laminar convective flow in the presence of transverse magnetic field with volume fraction and chemical reaction between non-conducting walls. In recent years, many researches [13], [14] and [15] contributes on the influence of heat transfer on dusty fluid as it is one of the thrust area. K.R. Madhura and G. Kalpana [16] have discussed the thermal effect on unsteady, visco-elastic, incompressible dusty fluid flow under pulsatile pressure gradient between two parallel plates. The effects of heat generation or absorption on non-uniform single and double slot suctions or injections into a mixed convective unsteady flow a vertical stretching sheet are discussed numerically by R. Ravindran and N.Samyuktha [17]. Yanhai lin et al. [18] studied the internal heat source effect on momentum and heat transfer on a thin finite power-law liquid flim with the aid of numerical techniques.

The unsteady, laminar flow of a dusty fluid in porous medium through different channels was examined by several authors [19] to [22]. In particular, the study different channels was examined by several authors of irregular channel is significant in constructing dam across an open channel, irrigation systems, sewer system, industrial waste water applications, etc. The influence of free convective heat and mass transfer analysis with time dependent convective cooling and varying mass diffusion on Couette flow in an irregular channel have examined by R. Sivaraj and B. Rushi Kumar [23] and [24]. The close observation of the literature encourages to continue the work on study of flow pattern of unsteady, laminar, dusty fluid under pulsatile pressure gradient through irregular channel in porous medium. Further the main goal is to construct a

mathematical model of heat transfer on dusty fluid to examine the effect of various physical parameters on velocity, temperature and concentration. The coupled partial differential equations governing the flow have been solved both analytically and numerically. The outcomes expected to be more applicable to realistic engineering problems.

## **Nomenclature:**

u - velocity of the fluid phase

v - velocity of the dust phase

t - time;

 $\rho$  - density of the fluid

p - pressure of the fluid

x - co-ordinate axis along the channel

y - co-ordinate axis normal to the channel

 $\beta_T$  - thermal expansion coefficient

T - temperature of the fluid

 $T_w$  - wall temperature

 $C_w$  - wall concentration

 $\lambda$  - visco elastic parameter

N - number density of the dust particles

 $Q_1$  - volumetric rate of heat generation/absorption

 $\eta$  - permeability of the porous medium

m - mass per unit volume of the dust particles

v - kinematic viscosity

 $k_1$  - wave number

Grashof number:  $G_r = \frac{g\beta h(T_w - T_0)}{\gamma}$ 

visco-elastic parameter:  $V_e = \frac{\gamma \lambda}{h^2}$ ,

Relaxation time parameter  $\tau = \frac{mv}{kh^2}$ 

Prandtl number:  $P_r = \frac{\mu C_p}{K_T}$ 

Schmidt number:  $S_c = \frac{v}{D}$ 

Thermal diffusion parameter  $T_d = \frac{D_T}{D} \left( \frac{T_W - T_0}{C_W - C_0} \right)$ 

Mass concentration of dust particle  $l = \frac{mN}{\rho}$ .

 $h_f$  - heat transfer coefficient

 $k_2$  - thermal conductivity of the fluid

A - positive real constant

h - width of the channel

 $K_T$  - coefficient of thermal conductivity of the fluid

 $D_T$  - coefficient of thermal diffusion

g - acceleration due to gravity

 $\beta_C$  - concentration expansion coefficient

 $K_T$  - concentration of the fluid

 $T_0$  - local temperature

 $C_0$  - local concentration

k - stokes resistance coefficient

 $C_p$  - specific heat at constant pressure

D - mass diffusivity (mass diffusion rate)

lpha - chemical reaction parameter

 $\varepsilon$  - amplitude parameter

 $u_0$  - constant

 $\mu$  - viscosity of the fluid =  $v\rho$ 

Solutal Grashof number:  $G_m = \frac{g\beta h(C_w - C_0)}{\gamma}$ ,

permeability coefficient of porous medium  $M = \frac{\eta}{h^2}$ 

Hartmann number  $Ha = B_0 h \sqrt{\frac{\sigma}{v}}$ 

heat source or sink parameter  $H_s = \frac{Q_1 h^2}{K_T}$ 

dimensionless chemical reaction parameter  $C_r = \frac{\alpha h^2}{\nu}$ 

Biot number  $B_i = \frac{h_f h}{K_T}$ 

### 2. Mathematical Model:

The study is restricted to an unsteady, viscous, laminar, convective heat and mass transfer flow of electrically conducting fluid between flat and wavy walls through porous medium. The constant magnetic field is applied in the direction of y-axis. The x-axis is taken in the direction along the walls which is set in motion and the y-axis is normal to the walls as shown in fig. 1. The wavy wall  $(y = \varepsilon \cos(k_1 x))$  has the temperature  $T_{w_1}$  which represents the convective boundary condition  $-K_T \frac{\partial T}{\partial y} = h_f [T_0 - T + (T_w - T_0)At]$  and concentration  $C_{w_1} = C_0 + (C_w - C_0)At$  respectively.

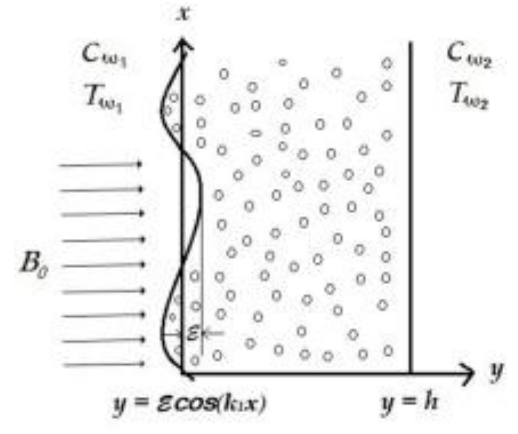


Figure 1: Geometry of the flow

The flat wall (y = h) has the temperature  $T_{w_2}$  which represents the convective boundary condition  $-K_T \frac{\partial T}{\partial v} = h_f [T_w - T + (T_w - T_0)At]$  and concentration  $C_{w_2} = C_w + (C_w - C_0)At$  respectively. In the flow field, the temperature gradient is sufficient to cause natural convection. A pulsatile pressure gradient is also imposed so that this resultant flow is a mixed convection flow. In the absence of extraneous force flow is unidirectional along the x-axis which is assumed to be infinite. In the porous region, the Brinkman - Darcy model which accounts for the inertia and boundary effects has been used for the momentum equation.

Based on the above assumptions the governing equations are

$$\frac{\partial u}{\partial t} = -\frac{1}{\rho} \frac{\partial p}{\partial x} + g \beta_T (T - T_0) + g \beta_C (C - C_0) - \frac{\sigma}{\rho} B_0^2 u + \gamma \left( 1 - \lambda \frac{\partial}{\partial t} \right) \frac{\partial^2 u}{\partial y^2} + \frac{kN}{\rho} (v - u) - \frac{\nu}{k} u, \tag{1}$$

$$\frac{\partial v}{\partial t} = \frac{k}{m} (u - v)$$

$$\frac{\partial T}{\partial t} = \frac{k_T}{\rho C_p} \frac{\partial^2 T}{\partial y^2} - \frac{Q_1}{\rho C_p} (T - T_0)$$
(3)

$$\frac{\partial v}{\partial t} = \frac{k}{m} (u - v) \tag{2}$$

$$\frac{\partial T}{\partial t} = \frac{K_T}{\rho C_n} \frac{\partial^2 T}{\partial y^2} - \frac{Q_1}{\rho C_n} (T - T_0) \tag{3}$$

$$\frac{\partial C}{\partial t} = D \frac{\partial^2 C}{\partial y^2} - \alpha (C - C_0) + D_T \frac{\partial^2 T}{\partial y^2}$$
 (4)

The initial and boundary conditions of temperature, concentration and velocity profiles are given by

i. When 
$$t=0$$
,  $u=0=v$ ,  $T=T_0$  and  $C=C_0$  for  $y\in (\varepsilon\cos(k_1x),h)$ 

ii. When 
$$t > 0$$
,  $u = 0 = v$ ,  $-K_T \frac{\partial T}{\partial y} = h_f [T_0 - T + (T_w - T_0)At]$ ,

$$C = C_0 + (C_w - C_0)At$$
 for  $y = \varepsilon \cos(k_1 x)$  and

$$C = C_0 + (C_w - C_0)At$$
 for  $y = \varepsilon \cos(k_1 x)$  and  $u = u_p = v$ ,  $-K_T \frac{\partial T}{\partial y} = h_f [T_w - T + (T_w - T_0)At]$  and  $C = C_w + (C_w - C_0)At$  for  $y = h$ .

To obtain the non-dimensional form of the above equations, following dimensionless parameters are used 
$$p^* = \frac{pu_0}{v\rho h}, \quad y^* = \frac{y}{h}, \quad x^* = \frac{x}{h}, \quad u^* = \frac{u}{u_0}, \quad v^* = \frac{v}{u_0}, \quad t^* = \frac{vt}{h^2}, \quad u_p^* = \frac{u_p}{u_0},$$

$$a^* = \frac{ah^2}{\gamma}, \quad \lambda_1 = k_1 h, \quad T^* = \frac{T - T_0}{T_w - T_0} \quad and \quad C^* = \frac{C - C_0}{C_w - C_0}.$$
The non-dimensional equations of (1), (2), (3) and (4), after dropping the \* are as follows,

$$\frac{\partial u}{\partial t} = -\frac{\partial p}{\partial x} + G_r T + G_m C + \left(1 - V_e \frac{\partial}{\partial t}\right) \frac{\partial^2 u}{\partial v^2} + \frac{l}{\tau} (v - u) - Ha^2 u - \frac{u}{M}$$
 (5)

$$\frac{\partial v}{\partial t} = \frac{1}{\tau} (u - v) \tag{6}$$

$$\frac{\partial^2 T}{\partial v^2} - P_r \frac{\partial T}{\partial t} - H_s T = 0 \tag{7}$$

The non-dimensional equations of (1), (2), (3) and (4), after dropping the \* are as follows,
$$\frac{\partial u}{\partial t} = -\frac{\partial p}{\partial x} + G_r T + G_m C + \left(1 - V_e \frac{\partial}{\partial t}\right) \frac{\partial^2 u}{\partial y^2} + \frac{l}{\tau} (v - u) - Ha^2 u - \frac{u}{M} \tag{5}$$

$$\frac{\partial v}{\partial t} = \frac{1}{\tau} (u - v) \tag{6}$$

$$\frac{\partial^2 T}{\partial y^2} - P_r \frac{\partial T}{\partial t} - H_s T = 0 \tag{7}$$

$$\frac{\partial^2 C}{\partial y^2} - S_c \frac{\partial C}{\partial t} - C_r S_c C + T_d \frac{\partial^2 T}{\partial y^2} = 0$$
and the corresponding initial and boundary conditions reduces to following form.

and the corresponding initial and boundary conditions reduces to following form,

i. When 
$$t = 0$$
,  $u = 0 = v$ ,  $T = 0$  and  $C = 0$  for  $y \in (b, 1)$ 

i. When 
$$t=0$$
,  $u=0=v$ ,  $T=0$  and  $C=0$  for  $y\in(b,1)$   
ii. When  $t>0$ ,  $u=0=v$ ,  $\frac{\partial T}{\partial y}=B_i(T-t)$ ,  $C=t$  for  $y=b$  and

$$u = u_p = v$$
,  $\frac{\partial T}{\partial v} = B_i(T - 1 - t)$  and  $C = 1 + t$  for  $y = 1$ .

Where  $b = \varepsilon \cos(\lambda_1 x)$ .

## 3. Solution of the Problem:

## 3.1 Exact Solution:

On solving the equation (7) using the variable separable method, the temperature attained is

$$T = \frac{B_i t e^{m_1(y-b)}}{B_i - m_1} + \frac{B_i [1 - (e^{m_1(1-b)} - 1)t]}{2 \sinh(m_1(1-b))} \left( \frac{e^{m_1(y-b)}}{B_i - m_1} - \frac{e^{-m_1(y-b)}}{B_i + m_1} \right)$$
(9)

Where  $m_1 = \sqrt{c_1 P_r H_s}$ ,  $c_1 > 0$  is the variable separable constant. Laplace transform of C, u and v are given by  $L[C(t)] = \int_0^\infty e^{-st} C(t) dt$ ,  $L[u(t)] = \int_0^\infty e^{-st} u(t) dt$  and  $L[v(t)] = \int_0^\infty e^{-st} v(t) dt$ .

By substituting (9) in (8) and applying Laplace transform to the resulting equation and boundary conditions, one can obtain the following equation

$$\frac{d^2 \bar{C}}{dy^2} - m_2^2 \bar{C} = \frac{T_d B_i m_1^2}{2 \sinh (m_1 (1-b))} \left( \frac{1 - e^{m_1 (1-b)}}{s^2} + \frac{1}{s} \right) \left( \frac{e^{m_1 (y-b)}}{B_i - m_1} - \frac{e^{-m_1 (y-b)}}{B_i + m_1} \right) - \frac{T_d B_i m_1^2 e^{m_1 (y-b)}}{(B_i - m_1) s^2},$$

$$\bar{C} = \frac{1}{s^2} \text{ at } y = b \text{ and } \bar{C} = \frac{1}{s} + \frac{1}{s^2} \text{ at } y = 1.$$

By taking the inverse Laplace transformation to the above equation, the concentration is given by

$$C = [A_{1}t + A_{2}(y - b) + A_{3}]e^{\sqrt{C_{r}S_{c}}(y - b)} + (A_{4}t + A_{5})e^{m_{1}(y - b)} + (A_{6}t + A_{7})\sinh\left(\sqrt{C_{r}S_{c}}(1 - b)\right) + A_{8}(y - b)\cosh\left(\sqrt{C_{r}S_{c}}(1 - b)\right) + (A_{9}t + A_{10})\cosh\left(m_{1}(1 - b)\right) + +(A_{11}t + A_{12}) \times \sinh\left(m_{1}(1 - b)\right) + \sum_{n=1}^{\infty} D_{n}e^{-C_{8}t}\sin\left(\frac{n\pi(y - b)}{1 - b}\right)$$

$$(10)$$

Let the pulsatile pressure gradient to be imposed on the system for t > 0. So we can write

$$-\frac{\partial P}{\partial x} = P_0(1 + \alpha \cos \beta t),$$

Where  $P_0$  is constant.

The Laplace transform of the equation (5) and (6), after using (9) and (10) are given by
$$s\bar{u} = P_0 \left( \frac{1}{s} + \frac{\alpha s}{s^2 + \beta^2} \right) + G_r B_i \left[ \frac{1}{2 \sinh (m_1(1-b))} \left( \frac{1-e^{m_1(1-b)}}{s^2} + \frac{1}{s} \right) \left( \frac{e^{m_1(y-b)}}{B_i - m_1} - \frac{e^{-m_1(y-b)}}{B_i + m_1} \right) \right.$$

$$\left. + \frac{e^{m_1(y-b)}}{(B_i - m_1)s^2} \right] + G_m \left[ e^{\sqrt{C_r S_c}(y-b)} \left( \frac{A_1}{s^2} + \frac{A_2(y-b) + A_3}{s} \right) + e^{m_1(y-b)} \left( \frac{A_4}{s^2} + \frac{A_5}{s} \right) + \sinh \left( \sqrt{C_r S_c} (1-b) \right) \right.$$

$$\left. \times \left( \frac{A_6}{s^2} + \frac{A_7}{s} \right) + \frac{A_8(y-b)}{s} \cosh \left( \sqrt{C_r S_c}(y-b) \right) + \cosh(m_1(y-b)) \left( \frac{A_9}{s^2} + \frac{A_{10}}{s} \right) + \sinh(m_1(1-b)) \right.$$

$$\left. \times \left( \frac{A_{11}}{s^2} + \frac{A_{12}}{s} \right) + \sum_{n=1}^{\infty} \frac{D_n}{s + C_8} \sin \left( \frac{n\pi(y-b)}{1-b} \right) + (1 - V_e s) \frac{d^2\bar{u}}{dy^2} + \frac{l}{\tau} (\bar{v} - \bar{u}) - \left( Ha^2 + \frac{1}{M} \right) \bar{u},$$

$$(11)$$

$$s\bar{v} = \frac{1}{\tau}(\bar{u} - \bar{v}),\tag{12}$$

Where  $m_2 = \sqrt{S_c(s + C_r)}$ .

The transformed boundary conditions are

$$\bar{u} = 0 = \bar{v}$$
 at  $y = b$  and

$$\bar{u} = \frac{u_p}{s} = \bar{v}$$
 at  $y = 1$  (13)

Equation (12) implies

$$\bar{v} = \frac{\bar{u}}{1+sr}.\tag{14}$$

$$\begin{split} & \bar{v} \text{ can be eliminated from the equation (11) with the help of (14) and it has reduced to} \\ & \bar{v} \text{ can be eliminated from the equation (11) with the help of (14) and it has reduced to} \\ & \frac{d^2 \bar{u}}{dy^2} - Q^2 \bar{u} = -\frac{1}{1 - V_e s} \Big\{ P_0 \left( \frac{1}{s} + \frac{\alpha s}{s^2 + \beta^2} \right) + G_r B_i \left[ \left( \frac{1 - e^{m_1(1-b)}}{s^2} + \frac{1}{s} \right) \left( \frac{e^{m_1(y-b)}}{B_i - m_1} - \frac{e^{-m_1(y-b)}}{B_i + m_1} \right) \right. \\ & \times \frac{1}{2 \sinh \left( m_1(1-b) \right)} + \frac{e^{m_1(y-b)}}{\left( B_i - m_1 \right) s^2} \Big] + G_m \left[ e^{\sqrt{C_r S_c}} (y-b) \left( \frac{A_1}{s^2} + \frac{A_2(y-b) + A_3}{s} \right) + e^{m_1(y-b)} \left( \frac{A_4}{s^2} + \frac{A_5}{s} \right) \right. \\ & + \sinh \left( \sqrt{C_r S_c} (1-b) \right) \left( \frac{A_5}{s^2} + \frac{A_7}{s} \right) + \frac{A_8(y-b)}{s} \cosh \left( \sqrt{C_r S_c} (y-b) \right) + \cosh \left( m_1(y-b) \right) \left( \frac{A_9}{s^2} + \frac{A_{10}}{s} \right) \\ & + \sinh \left( m_1(1-b) \right) \left( \frac{A_{11}}{s^2} + \frac{A_{12}}{s} \right) + \sum_{n=1}^{\infty} \frac{D_n}{s + C_8} \sin \left( \frac{n\pi(y-b)}{1-b} \right) \Big] \Big\} \\ & \text{Where } Q^2 = \frac{1}{1 - V_e s} \Big\{ s + \frac{sl}{1 + s\tau} + Ha^2 + \frac{1}{M} \Big\} \,. \end{split}$$

By imposing inverse Laplace transform to  $\bar{u}$  and  $\bar{v}$ , the fluid and dust velocities are obtained as follows,  $u = (A_{13}t + A_{14}) \sinh(\alpha_1(y - b)) + \sum_{n=1}^{\infty} E_n(t) \sin(\frac{n\pi(y-b)}{1-b}) + (A_{15}t + A_{16})(e^{\alpha_1(y-b)} - e^{m_1(y-b)}) + A_{17}(y - b)e^{\alpha_1(y-b)} + (A_{18}t + A_{19}) \sinh(m_1(y - b)) + (A_{20}t + A_{21})[e^{\alpha_1(y-b)} - \cosh(m_1(y - b))]$  $+(A_{22}e^{y_3t}+A_{23}e^{y_4t}+A_{24}t+A_{25})\sinh\left(\sqrt{C_rS_c}(y-b)\right)+(A_{26}e^{y_3t}+A_{27}e^{y_4t}+A_{28})(y-b)$  $\times e^{\sqrt{C_r S_c}(y-b)} + (A_{29}t + A_{30}) \left( e^{\alpha_1(y-b)} - e^{\sqrt{C_r S_c}(y-b)} \right) + (A_{31}e^{y_3t} + A_{32}e^{y_4t} + A_{35})(y-b)$ 

$$\times \cosh\left(\sqrt{C_r S_c}(y-b)\right) + A_{34}(y-b)\cosh\left(\alpha_1(y-b)\right) + \frac{P_0}{\alpha_1^2}\left(1 - e^{\alpha_1(y-b)}\right) + [f_1(y)C_2f_2(y)C_3]$$

$$-f_3(y)C_4 - f_4(y)C_5[A_{36}\cos(\beta t) + A_{37}\sin(\beta t)][f_1(y)C_3 - f_2(y)C_2 + f_3(y)C_5 - f_4(y)C_4]$$

 $\times (A_{37}\cos(\beta t) - A_{36}\sin(\beta t))$ ,

And

$$v = (A_{13}t + A_{38})\sinh(\alpha_{1}(y - b)) + \sum_{n=1}^{\infty} F_{n}(t)\sin(\frac{n\pi(y - b)}{1 - b}) + (A_{15}t + A_{39})(e^{\alpha_{1}(y - b)} - e^{m_{1}(y - b)})$$

$$+A_{17}(y - b)e^{\alpha_{1}(y - b)} + (A_{18}t + A_{40})\sinh(m_{1}(y - b)) + (A_{20}t + A_{41})[e^{\alpha_{1}(y - b)} - \cosh(m_{1}(y - b))]$$

$$+(A_{42}e^{y_{3}t} + A_{43}e^{y_{4}t} + A_{24}t + A_{44})\sinh(\sqrt{C_{r}S_{c}}(y - b)) + (A_{45}e^{y_{3}t} + A_{46}e^{y_{4}t} + A_{28})(y - b)$$

$$\times e^{\sqrt{C_{r}S_{c}}(y - b)} + (A_{29}t + A_{47})(e^{\alpha_{1}(y - b)} - e^{\sqrt{C_{r}S_{c}}(y - b)}) + (A_{48}e^{y_{3}t} + A_{49}e^{y_{4}t} + A_{35})(y - b)$$

$$\times \cosh(\sqrt{C_{r}S_{c}}(y - b)) + A_{34}(y - b)\cosh(\alpha_{1}(y - b)) + \frac{P_{0}}{\alpha_{1}^{2}}(1 - e^{\alpha_{1}(y - b)}) + [f_{1}(y)C_{2} + f_{2}(y)C_{3}$$

$$-f_{3}(y)C_{4} - f_{4}(y)C_{5}](A_{50}\cos(\beta t) + A_{51}\sin(\beta t))[f_{1}(y)C_{3} - f_{2}(y)C_{2} + f_{3}(y)C_{5} - f_{4}(y)C_{4}]$$

$$\times (A_{51}\cos(\beta t) - A_{50}\sin(\beta t)), \tag{15}$$

### 3.2 Numerical Solution:

The Crank Nicolson approximation of temperature (7) and concentration (8) are given by

$$\frac{1}{2h_{1}^{2}} \left( T_{j-1,n} - 2T_{j,n} + T_{j+1,n} + T_{j-1,n+1} - 2T_{j,n+1} + T_{j+1,n+1} \right) - \frac{P_{r}}{h_{2}} - H_{s} T_{j,n} = 0, \tag{16}$$

$$\frac{1}{2h_{1}^{2}} C_{j-1,n+1} - \left( \frac{1}{2h_{1}^{2}} + \frac{S_{c}}{h_{2}} \right) C_{j,n+1} + \frac{1}{2h_{1}^{2}} C_{j+1,n+1} = -\frac{1}{2h_{1}^{2}} C_{j-1,n} + \left( \frac{1}{h_{1}^{2}} - \frac{S_{c}}{h_{2}} + C_{r} S_{c} \right) C_{j,n} - \frac{1}{2h_{1}^{2}} C_{j-1,n} - \frac{T_{d}}{2h_{1}^{2}} \left( T_{j-1,n} - 2T_{j,n} + T_{j+1,n} + T_{j-1,n+1} - 2T_{j,n+1} + T_{j+1,n+1} \right) \tag{17}$$

The fluid and dust velocities are approached by finite difference method for (5) and (6) which is as follows:  $\frac{u_{j,n+1}-u_{j,n}}{h_2} = P_0(1+\alpha\cos(nh_2\beta)) + G_rT_{j,n} + G_mC_{j,n} + \frac{u_{j-1,n}-2u_{j,n}+u_{j+1,n}}{l} - \frac{V_e}{lk^2} \left[u_{j+1,n+1} - u_{j+1,n}\right]$ 

$$\frac{u_{j,n+1}-u_{j,n}}{h_2} = P_0(1+\alpha\cos(nh_2\beta)) + G_rT_{j,n} + G_mC_{j,n} + \frac{u_{j-1,n}-2u_{j,n}+u_{j+1,n}}{l} - \frac{V_e}{lk^2} \left[ u_{j+1,n+1} - u_{j+1,n} \right]$$

$$-2(u_{j,n+1}-u_{j,n})+u_{j-1,n+1}-u_{j-1,n}]+\frac{l_1}{\tau}(v_{j,n}-u_{j,n})-Ha^2u_{j,n}-\frac{u_{j,n}}{M},$$
(18)

$$\frac{v_{j,n+1} - v_{j,n}}{h_0} = \frac{u_{j,n} - v_{j,n}}{\tau}.$$
(19)

The corresponding boundary condition changes to

ii. when 
$$t > 0$$
,  $u_{0,n} = 0 = v_{0,n}$ ,  $\frac{T_{1,n} - T_{0,n}}{h_1} = B_i (T_{0,n} - nh_2)$  and  $C_{0,n} = nh_2$ , and

$$u_{n1,n} = u_p = v_{n1,n}$$
,  $\frac{T_{n1+1,n} - T_{n1,n}}{h_1} = B_i (T_{n1,n} - 1 - nh_2)$  and  $C_{n1,n} = 1 + nh_2$  for all values of  $n$ 

i. when t=0,  $u_{j,0}=0=v_{j,0}$ ,  $T_{j,0}=0$ ,  $C_{j,0}=0$  for all values of jii. when t>0,  $u_{0,n}=0=v_{0,n}$ ,  $\frac{T_{1,n}-T_{0,n}}{h_1}=B_i\big(T_{0,n}-nh_2\big)$  and  $C_{0,n}=nh_2$ , and  $u_{n1,n}=u_p=v_{n1,n}$ ,  $\frac{T_{n1+1,n}-T_{n1,n}}{h_1}=B_i\big(T_{n1,n}-1-nh_2\big)$  and  $C_{n1,n}=1+nh_2$  for all values of n, Where j refers to j with step size  $h_1=0.002$  and n refers to time t with its mesh  $h_2$ . Therefore, solutions of temperature, concentration, fluid and dust velocities are obtained from (16) to (19), and to study its behavior, numerical computation is examined for different values of the physical parameters that describe the flow characteristics and the results are exhibited graphically. The values of parameters are taken to be fixed as follows:  $u_p = 0.5$ ,  $K_T = 0.01$ ,  $\mu = 0.01$ ,  $h_f = 0.5$ ,  $\tau = 0.02$ . k = 0.05. The results have obtained by fixing  $h_1$  to 0.002 and to judge the accuracy of the convergence and stability of numerical techniques, the outcomes have computed with smaller values of  $h_1$  i.e.,  $h_1 = 0.0001$ , 0.0005, etc, and no considerable changes was observed in each cases.

### 4. Results and Discussions:

Analytical and numerical solutions for temperature, concentration and velocities of fluid and dust phase for various physical parameters are discussed and exhibited graphically as shown in figures 2 to 17. Variation of temperature for disparate values of Biot number, Prandtl number and heat source or sink parameter are shown in fig. 2 to 4. Heat transfer can be analyzed with the assist of Biot number, as it raises, temperature falls since the resistance of heat transfer at the wall of the channel falls which is shown in fig. 2. When  $B_i \ll 1$ , the system is thermally simple, because of uniform temperature fields inside the system. When Biot number is smaller than 0.1, heat conduction inside the system is comparatively faster than the heat convection away from its surface. The temperature gradients are negligibly small inside the system. Since the temperature raises with its amount of thermal energy in the body, which in turn determines the rate of heat transfer into or out of it. The substantial decrease in temperature corresponds to cooling of the surface. Fig. 3 reveals that small augment in Prandtl number from 0.5 (for mixtures of noble gases), 0.63 (for oxygen) and 0.71 (for air) results in significant decline in temperature since thermal boundary layer thickness reduces. It is noticed from fig. 4, temperature increases when heat source or sink parameter increases.

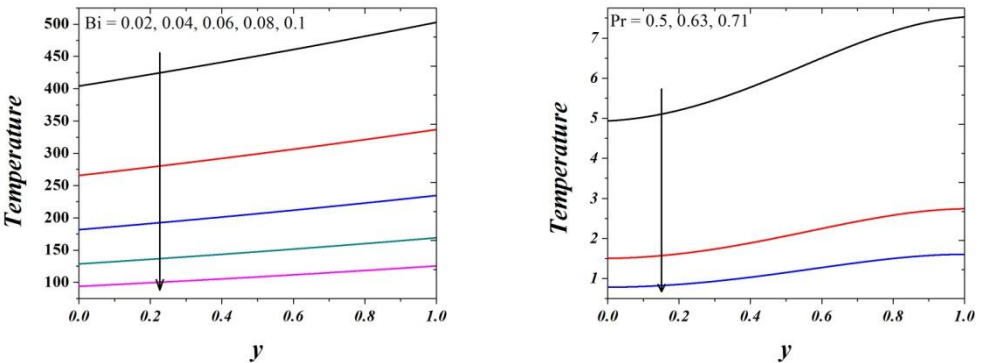


Figure 2, 3: Variation of temperature with Biot number and Prandtl number

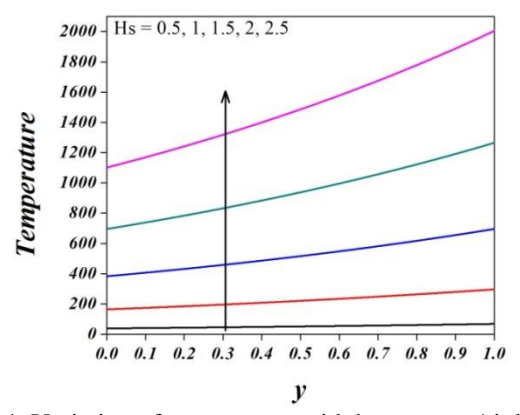


Figure 4: Variation of temperature with heat source/sink parameter.

With the help of fig. 5 to 8, the effects of concentration have been analyzed. Its evident that, concentration is directly proportional to heat source or sink parameter whereas inversely proportional to Schmidt number, Prandtl number and chemical reaction parameter. The Schmidt number taken for the study is 0.22, 0.6, 0.78 and 0.96 which physically corresponds to hydrogen, water vapor, ammonia and carbon dioxide respectively. As Schmidt number raises, conduction also raises which results in fallen in mass transfer, hence considerable reduction in concentration is observed. When Prandtl number elevated from 0.5 to 7 (for water at  $20^{\circ}C$ ), fallen in magnitude of concentration is noticed in fig. 7. Fig. 8 indicates that diffusion rate is affected by the chemical reaction, therefore concentration is reducing for higher values of chemical reaction parameter. Also, concentration is parabolic in nature for low Prandtl number and it is linear for high Prandtl number. Whereas it is linear for low chemical reaction parameter and parabolic for high chemical reaction parameter.

For various values of physical parameters, the velocity distribution of fluid and dust particles are elucidated graphically in fig. 9 to 16. One can conclude from fig. 9 that there is destruction in the velocity of fluid and dust when chemical reaction parameter enlarges. As expected, velocity reduces for higher values of Hartmann number, shown in fig, 10. This is due to the fact that when magnetic field is applied normal to the flow it slow down the movement of the fluid and dust in the channel. In addition, whenever Prandtl number and Schmidt number expands, velocity weakens which is depicted in fig. 11 and 12. On the other hand, velocity of fluid and dust increases with thermal diffusion parameter which is observed in fig. 13. Grashof number is the ratio of the buoyancy to viscous force acting on the fluid. Hence, velocity expands when increase in Grashof number due to the enhancement in buoyancy force. Reverse process is observed of solutal Grashof number which is shown in fig. 14 and 15. Also fig. 16 shows, the permeability of porous medium is directly proportional to the magnitude of velocities of dusty fluid. In all the cases one can noticed that as relaxation time of the dust particles decreases then the velocity of both fluid and dust become same. Also we observe that dust particles reaches the steady state slower than the fluid particles. This difference is due to the fact that the pulsatile pressure gradient is directly exerted on the fluid. Here, one can clearly see the effect of wavy wall on the velocity profiles of all physical parameters. The decrease in the magnitude of velocity profiles near to the wavy wall is proportional to the amplitude of the wavy wall. The fluid and dust velocities depends on frequency parameter and length of the wavy wall.

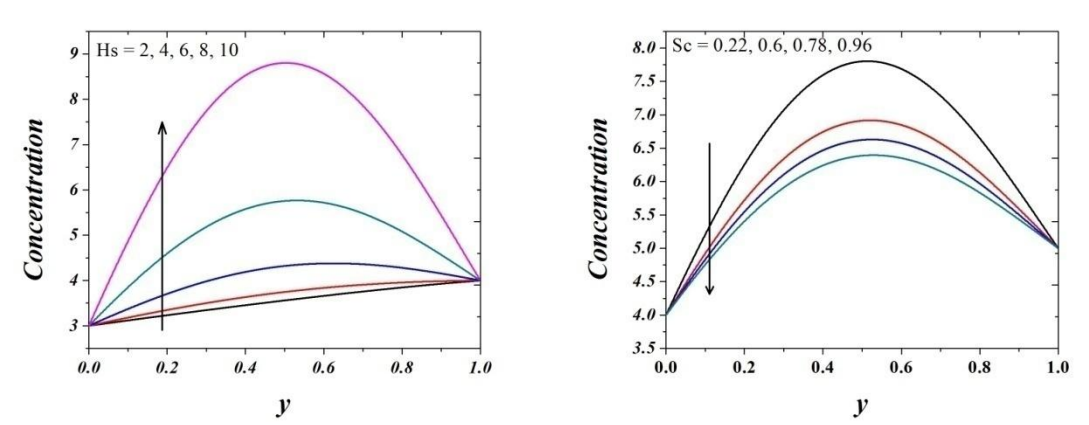


Figure 5, 6: Variation of concentration with heat source/sink parameter and Schmidt number

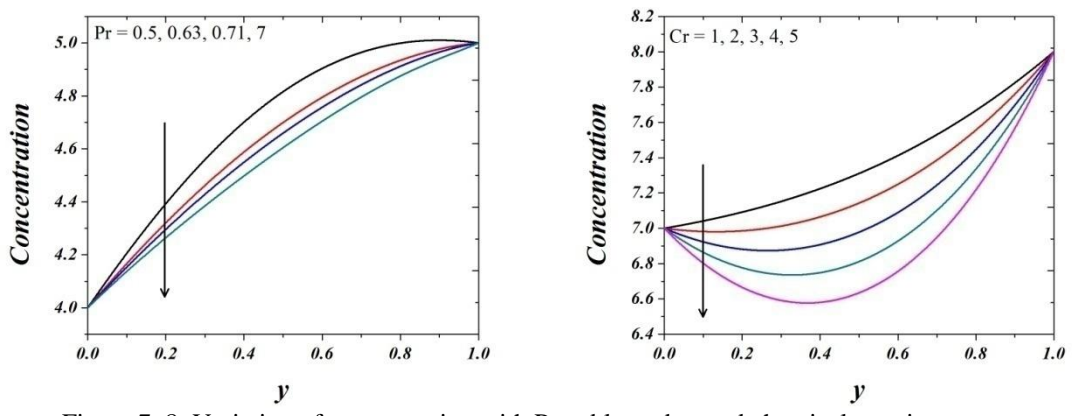


Figure 7, 8: Variation of concentration with Prandtl number and chemical reaction parameter

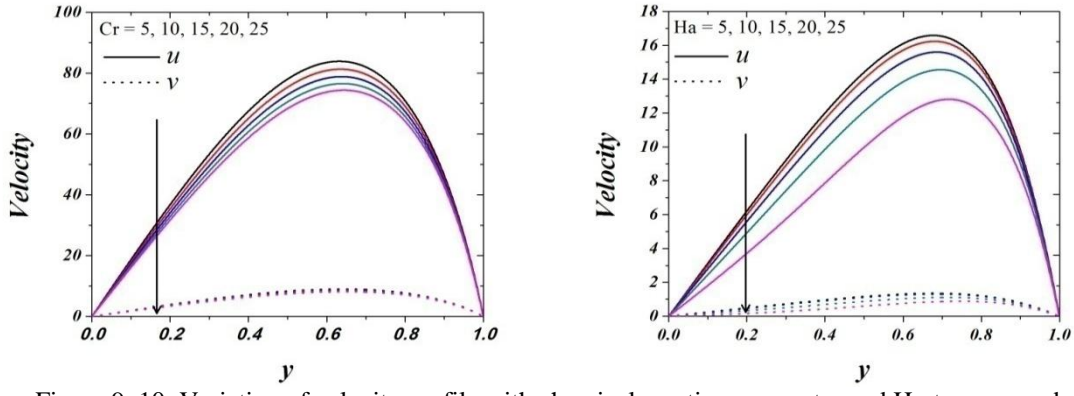


Figure 9, 10: Variation of velocity profile with chemical reaction parameter and Hartmann number

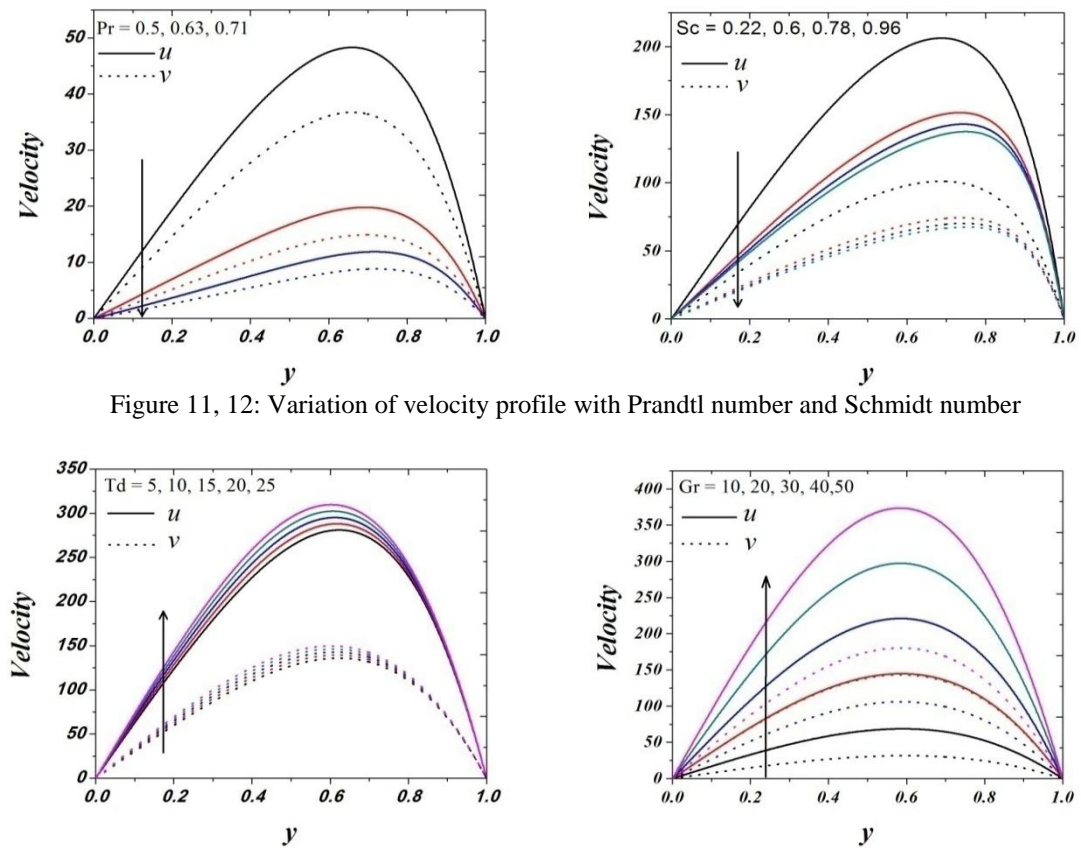


Figure 13, 14: Variation of velocity profile with thremal diffusion parameter and Grashof number

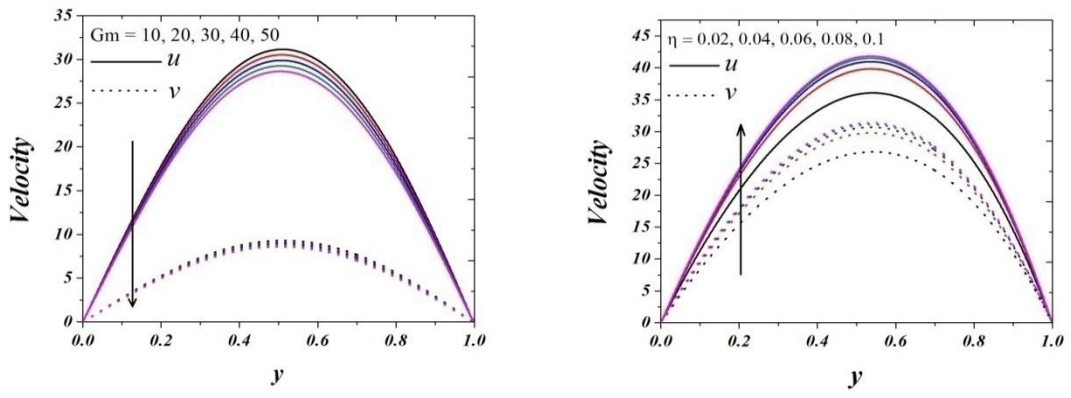


Figure 15,16: Variation of velocity profile with solutal Grash of number and permeability of the porous medium

### 5. Conclusions:

The effect of the temperature, concentration and velocities are discussed and shown graphically. The following conclusions are given by the influence of study of different physical parameters,

- Temperature near the wavy wall is least and maximum near the flat wall.
- ✓ Velocities are parabolic in nature and high in the middle of the channel.
   ✓ Concentration and velocities are less at the wavy than the non-wavy boundary.
   ✓ Dust velocity is less than fluid since dust particles restrict the flow.
- ✓ Both analytical and numerical solutions for temperature, concentration, fluid and dust velocities are exhibited in the tables 1 to 3. Although exact solutions are useful to get accurate results, it is time consuming and solving techniques are difficult. Therefore, the effort is made to find numerical results with the help of mathematical tool matlab and it have good agreement with analytical results.

Table 1: Comparison of exact and numerical solutions for velocity profiles.

у	For $P_r = 0.71$				For $C_r = 5$			
	$u_e$	$u_n$	$v_e$	$v_n$	$u_e$	$u_n$	$v_e$	$v_n$
0	0	0	0	0	0	0	0	0
0.2	3.4624	3.4846	2.4605	2.4822	36.7194	36.7795	3.8527	3.8714
0.4	7.1984	7.2110	5.2211	5.2217	67.4638	67.5069	7.1284	7.1637
0.6	10.5530	10.5693	7.7385	7.7790	83.4628	83.5011	8.9118	8.9528
0.8	10.8072	10.8210	8.0199	8.0711	70.8911	70.9248	7.6838	7.7138
1	0.5	0.5	0.5	0.5	0.5	0.5	0.5	0.5
у	For $S_c = 0.6$				For $H_a = 5$			
	$u_e$	$u_n$	$v_e$	$v_n$	$u_e$	$u_n$	$v_e$	$v_n = 0$
0	0	0	0	0	0	0	0	0
0.2	52.6200	52.6518	25.5412	25.6664	5.7138	5.7711	0.4463	0.4418
0.4	100.4237	100.5127	49.0168	49.0648	11.4984	11.5558	0.8695	0.8837
0.6	135.2187	135.4378	66.2534	66.2930	15.5132	15.5138	1.1911	1.2371
0.8	141.5167	141.5265	68.9110	69.4212	14.2954	14.3233	1.1348	1.4314
1	0.5	0.5	0.5	0.5	0.5	0.5	0.5	0.5
27	For $G_r = 30$				For $G_m = 30$			
У	$u_e$	$u_n$	$v_e$	$v_n$	$u_e$	$u_n$	$v_e$	$v_n$
0	0	0	0	0	0	0	0	0
0.2	102.6127	103.5111	66.1212	66.9715	17.1033	17.1768	5.0922	5.1104
0.4	181.9334	182.6894	117.9047	118.2116	28.0916	28.1433	8.4115	8.4122
0.6	211.4158	211.6004	137.1175	137.0000	28.4984	28.5236	8.5112	8.5447
0.8	161.1456	160.6456	105.3003	105.5946	17.8122	17.8385	5.2815	5.3222
1	0.5	0.5	0.5	0.5	0.5	0.5	0.5	0.5
у	For $S_c = 0.6$				For $H_a = 5$			
_	$u_e$	$u_n$	$v_e$	$v_n$	$u_e$	$u_n$	$v_e$	$v_n$
0	0	0	0	0	0	0	0	0
0.2	131.1458	131.2274	63.4519	63.4912	23.7118	23.7419	17.5001	17.8110
0.4	238.1260	238.8337	114.9649	115.6257	37.7514	37.7812	27.8012	27.9216
0.6	289.8235	290.1128	139.8888	140.3110	38.0511	38.0801	30.0112	30.2194
0.8	231.8528	232.0000	111.8119	112.2638	28.1749	28.1818	21.0811	20.1218
1	0.5	0.5	0.5	0.5	0.5	0.5	0.5	0.5

Table 2: Comparison of exact and numerical solutions of temperature

у	For $B_i = 0.1$		For I	$H_s = 2$	For $P_r = 0.71$		
	$T_e$	$T_n$	$T_e$	$T_n$	$T_e$	$T_n$	
0	94.0101	93.9134	726.6545	726.9345	0.7111	0.7811	
0.2	99.6823	99.5289	818.3123	818.4112	0.8001	0.8201	
0.4	105.7611	105.4810	922.1908	921.6879	0.9501	0.9711	
0.6	113.4945	111.7891	1039.1765	1038.0091	1.1911	1.2178	
0.8	120.3543	118.4745	1170.6667	1169.0081	1.4221	1.4411	
1	129.1233	125.5594	1319.5098	1316.1778	1.5720	1.6001	

Table 3: Comparison of exact and numerical solutions of temperature

Tuois of comparison of chart and numerical solutions of temperature								
у	For $H_s = 2$		For $P_r = 0.71$		For $C_r = 5$		For $S_c = 0.6$	
	$T_e$	$T_n$	$T_e$	$T_e$	$T_e$	$T_e$	$T_e$	$T_n$
0	3	3	4	4	7	7	4	4
0.2	3.2661	3.2333	4.2812	4.3011	6.6312	6.6701	5.7200	5.7216
0.4	3.4567	3.4542	4.5000	4.5521	6.5767	6.5845	6.7236	6.7427
0.6	3.6616	3.6612	4.7234	4.7658	6.7229	6.7601	6.8258	6.8409
0.8	3.8455	3.8459	4.8781	4.9119	7.2105	7.2237	6.1128	6.1327
1	4	4	5	5	8	8	5	5

### 5. References:

1. Om Prakash, Devendra Kumar and Y. K. Dwivedi, "Effects of thermal difffusion and chemical reaction on MHD flow of dusty visco-elastic (Walter's liquid model-B) fluid", J Electromagn Anal Appl, 2, 581-587, 2010.

- 2. E. Osalusi, J. Side and R. Harris, "Thermal diffusion and thermo effect on combined heat and mass transfer of a steady MHD convective and slip flow due to a rotating disk with viscous dissipation and ohmic heating", Int Commun Heat Mass Transfer, 35(8), 908-915, 2008.
- 3. A. Afify, "Similarity solution in MHD: Effects of thermal diffusion and diffusion thermo on free convective heat and mass transfer over a stretching surface considering suction or injection", Commun. Nonlinear Sci. Numer. Simul, 14(5), 2202-2214, 2009.
- 4. G. Palani and P. Ganesan, "Heat transfer effects on dusty gas flow past a semi-infinite inclined plate", Forsch ingenieurwes, 71, 223-230, 2007.
- 5. O. Anwar Beg, A. Y. Bakier and V. R. Prasad, "Numerical study of free convection magnetohydrodynamic heat and mass transfer from a stretching surface to a saturated porous medium with Soret and Dufour effects", Comput. Mater. Sci., 46, 57-65, 2009.
- 6. Rajesh sharma, R. Bhargava and Peeyush bhargava," A numerical solution of unsteady MHD convection heat and mass transfer past a semi-infinite vertical porous moving plate using element free Galerkin method", Comput. Mater. Sci., 48, 537-543, 2010.
- 7. B. J. Gireesha, G. K. Ramesh, H. J. Lokesh and C. S. Bagewadi, "Boundary layer flow and heat transfer of a dusty fluid over a stretching vertical surface", Appl. Math., 2, 475-481, 2011.
- 8. B. J. Gireesha, G. S. Roopa and C. S. Bagewadi, Boundary layer flow of an unsteady dusty fluid and heat transfer over a stretching sheet with non-uniform heat source/sink, Eng. 3, 726-735, 2011.
- 9. Krishnendu Bhattacharyya, "Effects of heat source/sink on MHD flow and heat transfer over a shrinking sheet with mass suction", Chem. Eng. Res. Bull., 15, 12-17, 2011.
- 10. P. V. S. Kamalakar, D. R. V. P. Rao and R. R. Rao, "Finite element analysis of chemical reaction effect on non-darcy convective heat and mass transfer flow through a porous medium in vertical channel with heat sources", Int. J. Appl. Math. Mech., 8(13), 13-28, 2012.
- 11. K. R. Madhura, Babitha and S. S. Iyengar, "Impact of heat and mass transfer on mixed convective flow of nanofluid through porous medium", Int. J. Appl. Comput. Math., https://doi.org/10.1007/s40819-017-0424-3, 1-24, 2017.
- 12. G. K. Ramesh and B. J. Gireesha, "Combined effects of non-uniform heat source/sink and radiation on heat transfer of a dusty fluid over a stretching sheet", Int. J Math. Archive, 3(4), 1429-1438, 2012.
- 13. P. Mohan krishna, V. Sugunamma and N. Sandeep, "Magnetic field and chemical reaction effects on convective flow of dusty viscous fluid", Commun. Appl. Sci., 1(1), 161-187, 2013.
- 14. Mustafa Turkyilmazoglu "Magnetohydrodynamic two-phase dusty fluid flow and heat model over deforming isothermal surfaces", Phy. Fluids, 29(1), 2017.
- 15. B. J. Gireesha, P. Venkatesh, N. S. Shashikumar, B. C. Prasannakumara, "Boundary layer flow of dusty fluid over a radiating stretching surface embedded in a thermally stratified porous medium in the presence of uniform heat source", Nonlinear Eng., 6(1), 31-41, 2017.
- 16. Karmina K. Ali, Hajar F. Ismael, Bewar A. Mahmood, Majeed A. Yousif, "MHD Casson fluid with heat transfer in a liquid film over unsteady stretching plate", Int. J. Adv. Appl. Sci., 4(1), 55-58, 2017.
- 17. K. R. Madhura and G. Kalpana, "Study of thermal effect on unsteady flow of a visco-elastic fluid under pulsatile pressure gradient", Int. J. Appl. Math. Sci., 7(1), 15-32, (2014)
- 18. R. Ravindran, N. Samyuktha, "Unsteady mixed convection flow over stretching sheet in presence of chemical reaction and heat generation or absorption with non-uniform slot suction or injection", Appl. Math. Mech., 36(10), 1253-1272, 2015.
- 19. Yanhai Lin, Liancun Zheng and Lianxi Ma, "Heat transfer characteristics of thin power-law liquid films over horizontal stretching sheet with internal heating and variable thermal coefficient", Appl. Math. Mech., 37(12), 1587-1596, 2016
- 20. K. R. Madhura, B. J. Gireesha and C. S. Bagewadi, "Exact solutions of unsteady dusty fluid flow through porous media in an open rectangular channel", Adv. theor. Appl. Mech., 2(1), 1-17, 2009
- 21. K. R. Madhura, B. J. Gireesha and C. S. Bagewadi, "Flow of an unsteady dusty fluid through porous media in a channel of triangular cross-section", Int. Rev. Phy, 4(6), 315-325, 2010
- 22. B. J. Gireesha, K. R. Madhura and C. S. Bagewadi, "Flow of an unsteady dusty fluid through porous media in a uniform pipe of a circle as cross-section", Int. J. Pure Appl. Math., 76(1), 29-47, 2012
- 23. M. Chipot, K. Kaulakyte, K. Pileckas and W. Xue, "On non homogeneous boundary value problems for the stationary Navier–Stokes equations in two-dimensional symmetric semi-infinite outlets", Anal. Appl., DOI: 10.1142/S0219530515500268, 1-27, 2015
- 24. R. Sivaraj and B. Rushi kumar, "Unsteady MHD dusty viscoelastic fluid couette flow in an irregular channel with varying mass diffusion", Int. J Heat Mass transfer, 55, 3076-3089, 2012
- 25. R. Sivaraj and B. Rushi kumar, "Chemically reacting dusty viscoelastic fluid flow in an irregular channel with convective boundary", Ain Shams Eng. J., 4, 93-101, 2013

## 6. Appendices:

$$\begin{split} &\alpha_1 = \sqrt{H_0^2 + \frac{1}{u_1}}, \quad &\alpha_2 = \frac{u(1+\gamma) + y_2(1+y_1)^2}{2x_1 N}, \quad &\alpha_3 = \frac{1}{1-y_2 V_2} \left( C_0 + \frac{C_{10}^2}{1+rC_{10}^2} + \alpha_1^2 \right), \\ &C_1 = \frac{T_0 B_1 m^2}{(x_1 - w_1)^2 - C_2 S_1}, \quad &C_2 = \sinh(R_1(1-b)) \cos(S_1(1-b)), \quad &C_3 = \cosh(R_1(1-b)) \sin(S_1(1-b)), \\ &C_4 = 1 - e^{R_1(1-b)} \cos(S_1(1-b)), \quad &C_5 = e^{R_1(1-b)} \sin(S_1(1-b)), \quad &C_6 = R + S V_0 \beta, \quad &C_7 = S - R V_0 \beta, \\ &C_8 = \frac{x^2 - x^2}{S_2(1-b)^2} + C_7, \quad &R = \frac{1}{1+v_2^2 \beta^2} \left( \frac{1}{M} - V_0 \beta^2 + H_0^2 + \frac{1}{1+y^2 \beta^2} \right), \quad &R_1 = \sqrt{\frac{y_1 + y_2 - y_2}{2^2}}, \\ &S = \frac{1}{1+v_2^2 \beta^2} \left( \frac{y_2}{M} + \beta(1 + V_0 H_0^2) + \frac{y_2 + y_2 - y_2}{1+y^2 \beta^2} \right), \quad &S_1 = \sqrt{\frac{y_1 + y_2 - y_2}{2}}, \quad &R_1 = \sqrt{\frac{y_1 + y_2 - y_2}{2^2}}, \\ &\times \cos(S_1(y-b)), \quad &f_2(y) = e^{R_1(y-b)} \sin(S_1(y-b)), \quad &f_3(y) = \sinh(R_1(y-b)) \cos(S_1(y-b)), \\ &f_1(y) = \cosh(R_1(y-b)) \sin(S_1(y-b)), \quad &G_9 = \sinh(m_1(1-b), \quad &G_{10} = 1 - e^{m_1(1-b)}, \\ &f_1(y) = \cosh(R_1(y-b)) \sin(S_1(y-b)), \quad &G_9 = \sinh(m_1(1-b), \quad &G_{10} = 1 - e^{m_1(1-b)}, \\ &G_{12} = \frac{1}{2} \left\{ \frac{y_2}{C_2}, \quad &G_{13} = \frac{x_1}{4} - \zeta_2, \quad &C_{14} = \sinh(\sqrt{C_1 S_2}(1-b), \\ &G_{12} = \frac{1}{2} \left\{ \frac{y_2}{C_2}, \quad &G_{13} = \frac{1}{2} - \frac{y_2}{C_2}, \quad &G_{12} = \frac{1}{2} - \frac{y_2}{C_2}, \\ &G_{17} = \cosh(R_1(y-b)) \sin(S_1(y-b)), \\ &G_{12} = \frac{1}{2} - \frac{y_2}{C_2} + \frac{y_2}{C_2} + \frac{y_2}{C_2} + \frac{y_2}{C_2} \right), \quad &G_{13} = \frac{1}{2} - \frac{y_2}{C_2} + \frac{y_2}{C_2} \right), \quad &G_{13} = \frac{1}{2} - \frac{y_2}{C_2} + \frac{y_2}{C_2} + \frac{y_2}{C_2} \right), \\ &G_{12} = \frac{1}{2} \left\{ \frac{y_2}{C_2}, \quad &G_{13} = \frac{1}{2} - \frac{y_2}{C_2} + \frac{y_2}{C_2} \right\}, \\ &G_{12} = \frac{1}{2} \left\{ \frac{y_2}{C_2}, \quad &G_{13} = \frac{1}{2} - \frac{y_2}{C_2} + \frac{y_2}{C_2} \right\}, \\ &G_{12} = \frac{1}{2} \left\{ \frac{y_2}{C_2}, \quad &G_{13} = \frac{y_2}{C_2} + \frac{y_2}{C_2} \right\}, \\ &G_{12} = \frac{y_2}{C_2} + \frac{y_2}{C_2} + \frac{y_2}{C_2} + \frac{y_2}{C_2} \right\}, \\ &G_{12} = \frac{y_2}{C_2} + \frac{y_2}{C_2} + \frac{y_2}{C_2} + \frac{y_2}{C_2} + \frac{y_2}{C_2} \right), \\ &G_{12} = \frac{y_2}{C_2} + \frac{y_2}{C_2} + \frac{y_2}{C_2} + \frac{y_2}{C_2} + \frac{y_2}{C_2} \right), \\ &G_{12} = \frac{y_2}{C_2} + \frac{y_2}{C$$

International Journal of Advanced Trends in Engineering and Technology (IJATET)
Impact Factor: 5.665, ISSN (Online): 2456 - 4664
(www.dvpublication.com) Volume 2, Issue 2, 2017

$$\begin{array}{l} A_{25} = -C_{24}G_{m}C_{23} \,, \quad A_{26} = \frac{1}{y_{3}-y_{4}} \Big[ q_{3}(y_{3}) + \frac{G_{m}A_{2}}{y_{3}q_{2}(y_{3})(1+\tau y_{3})^{2}} \Big], \quad A_{27} = \frac{1}{y_{3}-y_{4}} \\ \times \Big[ q_{3}(y_{4}) + \frac{G_{m}A_{2}}{y_{4}q_{2}(y_{4})(1+\tau y_{4})^{2}} \Big], \quad A_{28} = -A_{2}G_{m}C_{23} \,, \quad A_{29} = A_{1}G_{m}C_{23} \,, \quad A_{30} = G_{m}C_{23}[A_{3} + A_{1}V_{e}] \\ + 2\Big( A_{1}\alpha_{1}\alpha_{2} - A_{2}\sqrt{C_{r}S_{c}} \Big)C_{23} \Big], \quad A_{31} = \frac{A_{8}}{y_{3}(y_{3}-y_{4})} \Big[ q_{3}(y_{3}) + \frac{G_{m}}{q_{2}(y_{3})} \Big], \quad A_{32} = \frac{A_{8}}{y_{4}(y_{3}-y_{4})} \Big[ q_{3}(y_{4}) + \frac{G_{m}}{q_{2}(y_{4})} \Big], \\ A_{33} = (1-b)\alpha_{2}C_{18}C_{21} + V_{e} + 2\alpha_{1}\alpha_{2}C_{19} \,, \quad A_{34} = -\alpha_{1}C_{18}C_{21}(C_{22} - C_{21})(G_{r}C_{20} + G_{m}A_{4}) + \frac{\alpha_{2}}{m_{1}}G_{r}C_{10}C_{24} \\ \times \left[ B_{i} + m_{1}C_{9}(C_{17} - C_{22}) \right] + G_{m}\alpha_{2}C_{18}C_{23} \Big[ \frac{A_{6}C_{23}}{c_{14}} - A_{1}(C_{22} - C_{25}) \Big] + \alpha_{2}G_{m}A_{9}C_{18}C_{19}(C_{17} - C_{22}), \\ A_{35} = -G_{m}A_{8}C_{23} \,, A_{36} = \frac{\alpha_{P_{0}(c_{2}C_{6} - c_{3}C_{7})}{2!(c_{2}C_{6} - c_{3}C_{7})^{2} + (c_{2}C_{7} + c_{3}C_{6})^{2}} \Big], A_{37} = \frac{\alpha_{P_{0}(c_{2}C_{7} + c_{3}C_{6})}{2!(c_{2}C_{6} - c_{3}C_{7})^{2} + (c_{2}C_{7} + c_{3}C_{6})^{2}} \Big], \\ A_{38} = A_{14} + (C_{22} - C_{21})C_{9}C_{19}[G_{r}B_{i} + \tau A_{4}G_{m}(B_{i} - m_{1})] - \frac{G_{r}}{m_{1}}\tau B_{i}C_{10}C_{11}C_{18}C_{20} - \tau C_{18}C_{19}(C_{17} - C_{22}) \\ \times \left( \frac{G_{r}C_{10}C_{24}}{C_{19}} + A_{9} \right), \quad A_{39} = A_{16} - C_{19}[G_{r}B_{i} + \tau G_{m}A_{4}(B_{i} - m_{1})], \quad A_{40} = A_{19} - \frac{G_{r}}{m_{1}}\tau B_{i}C_{10}C_{24} + \tau A_{11}C_{19} \,, \\ A_{41} = A_{21} - \tau[G_{r}C_{10}C_{24} + A_{9}C_{19}], \quad A_{42} = \frac{A_{22}}{1 + \tau y_{3}}, \quad A_{43} = \frac{A_{23}}{1 + \tau y_{4}}, \quad A_{44} = A_{25} + \tau A_{6}C_{23}, \\ A_{45} = \frac{A_{26}}{1 + \tau y_{3}}, \quad A_{46} = \frac{A_{27}}{1 + \tau y_{4}}, \quad A_{47} = A_{30} - \tau A_{1}G_{m}C_{23}, \quad A_{48} = \frac{A_{31}}{1 + \tau y_{3}}, \quad A_{49} = \frac{A_{32}}{1 + \tau y_{4}}, \\ A_{50} = \frac{\alpha_{P_{0}(c_{2}C_{6} - c_{3}C_{7} - \tau \beta_{2}C_{6} - \tau \beta_{3}C_{6})^{2} + (c_{2}C_{7} - \tau \beta_{3}C_{6} - \tau \beta_{3}C_{6})^{2}}{2[(c_{2}C_{6} - c_{3}C_{7$$